Effects of Temperature and Swelling on Chain Dynamics during the Sol−Gel Transition

To Ngai,[†] Chi Wu,*[,†,‡] and Yun Chen[§]

Department of Chemistry, The Chinese University of Hong Kong, Shatin N.T., Hong Kong; The Open Laboratory of Bond Selective Chemistry, Department of Chemical Physics, University of Science and Technology of China, Hefei, Anhui, China; and Department of Chemical Engineering, National Cheng Kung University, Taiwan 70101

Received August 8, 2003; Revised Manuscript Received October 22, 2003

ABSTRACT: The UV-irradiation-induced [2 + 2] photocycloaddition of 7-methacryloyloxy-4-methylcoumarin attached to PMMA can transfer a semidilute solution to a homogeneous and speckle-free chemical gel. It allows us to study the effect of temperature on the chain dynamics at each stage of the sol−gel transition by laser light scattering. The fast and slow relaxation modes in semidilute solution are preserved in the resultant gel. For the fast mode, the characteristic decay time $\langle\tau_c\rangle_f$ and its related scattering intensity $\langle I\rangle_{fast}$ are nearly temperature-independent because it is related to the motions of the subchains ("blobs") between two cross-linked points. In contrast, $\langle\tau_c\rangle_s$ and $\langle I\rangle_{slow}$ increase as the temperature decreases from 40 to 10 °C, which cannot be attributed to the chain conformation because chloroform remains a good solvent in this temperature range. The increase of $\langle I\rangle_{slow}$ is because the lights scattered from the segments of different chains are more correlated at lower temperatures (higher viscosity). This study further supports that the slow mode is due to the density fluctuation. Moreover, the scattering vector (q) dependence of $\langle\tau_c\rangle_f$ and $\langle\tau_c\rangle_s$ shows that as the temperature decreases, the scaling exponent α_f in $1/\langle\tau_c\rangle_f \sim q^{\alpha_f}$ increases from 2.0 to 2.4, but α_s in $1/\langle\tau_c\rangle_s \sim q^{\alpha_s}$ decreases from 3.0 to 2.2, which can be related to the decrease of static correlation length. The swelling of the resultant gel shows a similar effect as the increase of the temperature.

Introduction

The dynamics of polymer chains in solution have always been an essential and important part of polymer science. Although the behaviors of individual isolated polymer chains in dilute solution under the Θ- and good-solvent condition are fairly understood, the slow dynamics (not the slow reptation of one chain in the maze of other chains) of polymer chains in semidilute and concentrated solution still remains an open question.[1] Because of the chain overlapping and entanglements, semidilute and concentrated solutions have a more complicate chain dynamics than dilute solution. It is not only difficult in real experiments, such as the sample preparation in laser light scattering (LLS), but also complicated in theoretical treatment and computer simulation because one has to deal with a multibody problem.[2] Over a very long period, we have had no good grip on characteristic properties of semidilute and concentrated solutions until the concept of "blobs" as well as the scaling and reptation theories were gradually introduced and developed.[3]

An important prediction of the scaling theory for semidilute solution made of linear flexible chains in good solvent is the existence of one characteristic length and, consequently, one dynamical relaxation process, characterized by the cooperative diffusion coefficient (D_c) of the subchains (blobs) between two neighboring entangled points. Experimentally, such a cooperative diffusive relaxation and its concentration dependence have been well confirmed. However, some additional dynamic processes were also observed, leading to a deviation of the intensity−intensity time correlation function ($G^{(2)}(q,\tau)$) measured in dynamic laser light scattering (LLS) from a single-exponential decay. Such a deviation becomes more pronounced when the Θ condition was approached.[4−7] Brown et al.[8] investigated a number of polystyrene semidilute solutions in good as well as Θ solvents and found that $G^{(2)}(q,\tau)$ has a distinct slow relaxation mode in addition to the fast mode assigned to the motions of the blobs. They showed that the characteristic line width (Γ_f) of the fast mode was proportional to the square of the scattering vector (q), but the slow mode was q-independent, which was attributed to the structural relaxation of a temporary network inside semidilute solution.

However, different controversial results related to the slow relaxation in semidilute solutions have also appeared in the literature.[9−12] For example, Koch et al.[10] found that the slow mode of short polyisoprene and polystyrene chains in semidilute solutions was diffusive, i.e., $\Gamma_s \propto q^2$, supported by other similar results.[1,11] Brown et al.[1] and Burchard[13] suggested that the dissolution process might result in an inhomogeneous network-like structure, or in other words, the overlapping of polymer chains in semidilute solution might lead to some "transient clusters". The translational motion of these "clusters" could result in such a slow diffusive behavior. Heckmeier et al.[11] attributed these "transient clusters" to physical association, but others thought that they might be the results of incomplete dissolution because only one relaxation mode was observed after a long-time dissolution.[8] It is helpful to note that due to the practical problem in the sample preparation, most of the past LLS studies used short polystyrene chains with a molar mass lower than 10^5 g/mol.

At this point, we like to remind readers that the slow relaxation in semidilute solution should not be mixed with other slow relaxation observed in polyelectro-

[†] The Chinese University of Hong Kong.
[‡] University of Science and Technology of China.
[§] National Cheng Kung University.
* To whom correspondence should be addressed at The Chinese University of Hong Kong.

10.1021/ma030421b CCC: $27.50
Published on Web 01/13/2004

lytes,[14,15] block copolymers,[16] polysaccharides,[17,18] and associating polymers[19,20] because they have completely different physical origins. It is expected that the chain dynamics of these polymers in semidilute solution would be even more complicated. Therefore, we would like to limit ourselves to the slow relaxation of linear flexible neutral chains in semidilute solutions at this moment because it is an essentially important starting point for the study of other more complicated polymer systems. Moreover, the dynamics of polymer chains in semidilute and concentrated solutions is a bridge between dilute solution and polymer melts. Therefore, more cleverly designed experiments are certainly needed to explore the nature of the slow relaxation in semidilute and concentrated solutions. Its significance in polymer science cannot be overemphasized.

Recently, we have reported the effects of concentration and cross-linking on the chain dynamics of poly(methyl methacrylate-*co*-7-methacryloyloxy-4-methylcoumarin) [P(MMA-*co*-AMC)] chains in semidilute chloroform solution.[21,22] The advantage of using such a system relies on the fact that the [2 + 2] photocycloaddition of the pendant photosensitive coumarin groups in the chain backbone under the UV irradiation of ~310 nm can result in a homogeneous and speckle-free chemical gel. It enables us to study the chain dynamics at each stage of the sol−gel transition so that we can monitor how the fast and slow relaxation modes in semidilute solutions are affected by the cross-linking. Our results showed that the characteristic line widths (Γ_f and Γ_s) of the fast and slow relaxation modes prior to the cross-linking were respectively scalable to the scattering vector q as $\Gamma_f \sim q^{\alpha_f}$ with $\alpha_f \approx 2.0 \pm 0.1$, the hallmark of a diffusive relaxation, and as $\Gamma_s \sim q^{\alpha_s}$ with $\alpha_s \approx 3.0 \pm 0.1$, the signature of internal motions.[21] As the cross-linking proceeds, α_s decreases from 3.0 to 2.3 because the static correlation length (ξ_{static}) measured in static LLS changed from $\xi_{static} > 1/q$ to $\xi_{static} \sim 1/q$.[22] In the present study, we extend our previous studies to the effects of the temperature and swelling on the fast and slow relaxation modes. It is helpful to note that such a temperature effect cannot be obtained during a conventional sol−gel transition. Here, our main objectives are to confirm that the slow relaxation is related to the thermally agitated density (concentration) fluctuation, and the value of α_s is attributed to the ratio of the LLS observation length ($1/q$) to ξ_{static}. In order words, $\alpha_s \to 2$ when $\xi_{static} \ll 1/q$, $\alpha_s \to 3$ when $\xi_{static} \gg 1/q$, and $2 < \alpha_s < 3$ when $\xi_{static} \sim 1/q$.

Experimental Section

Sample Preparation. 7-Hydroxy-4-methylcoumarin and methacryloyl chloride (Acros) were used without further purification. Methyl methacrylate (MMA, Aldrich) was purified by vacuum distillation. AIBN (Aldrich) was purified by recrystallization from methanol. *N*,*N*-Dimethylformamide (DMF) was purified by vacuum distillation after drying with barium oxide. Other solvents and chemicals were used as received. The synthesis of photoreactive copolymer P(MMA-*co*-AMC) involves two steps, and the details have been reported before.[21] The first step is to prepare 7-methacryloyloxy-4-methylcoumarin (AMC). 150 mL of chloroform was added to a solution of 7-hydroxy-4-methylcoumarin (12.0 g, 68 mmol) in 192 mL of 0.5 N NaOH aqueous solution and then cooled to 5 °C. Under vigorous stirring, methacryloyl chloride (7.1 g, 68 mmol) was injected into the mixture, and the reaction was continued for 1 h. The white solid obtained after evaporating solvents was recrystallized in acetone.[21,23] In the second step, AMC was copolymerized with methyl methacrylate (MMA) in DMF by using AIBN as initiator.[21,24] Freshly distilled MMA and AMC as well as AIBN solution were charged into a polymerization tube and the ratio of [MMA]:[AMC]:[AIBN] is 9:1:0.0002. After three freeze−thaw cycles of degassing, the tube was sealed off under vacuum. The reaction was carried at 60 °C for ~40 h. The resultant copolymer P(MMA-*co*-AMC) was harvested in methanol, purified, and dried overnight in a vacuum. The sample used has a weighted-averaged molar mass (M_w, LLS) of 2.1×10^5 g/mol with a polydispersity index (M_w/M_n, GPC) of 1.5 and contains 7.2 mol % of AMC estimated from NMR.

Laser Light Scattering. A commercial spectrometer (ALV/DLS/SLS-5022F) equipped with a multi-τ digital time correlator (ALV5000) and a cylindrical 22 mW UNIPHASE He−Ne laser ($\lambda_0 = 632$ nm) was used. The spectrometer has a high coherence factor of $\beta \sim 0.95$ because of a novel single-mode fiber optical coupled with an efficient avalanche photodiode (APD). In dynamic LLS, the intensity−intensity time correlation function ($G^{(2)}(q,\tau)$) [$= \langle I(q,0)I(q,\tau)\rangle$] of each copolymer solution at different photoreaction stages was measured in the scattering angle (θ) range 30°−150°. $G^{(2)}(q,\tau)$ can be related to the normalized field−field autocorrelation function $|g^{(1)}(q,\tau)|$ ($\equiv [\langle E(0)\, E^*(\tau)\rangle/\langle E(0)\, E^*(0)\rangle]$) via the Siegert relation as[25]

$$G^{(2)}(q,\tau) = \langle I(q,0)\rangle^2[1 + \beta|g^{(1)}(q,\tau)|^2]$$

or

$$G^{(2)}(q,\tau) \equiv \frac{G^{(2)}(q,\tau)}{\langle I(q,0)\rangle^2} - 1 = \beta|g^{(1)}(q,\tau)|^2 \qquad (1)$$

where $\langle I(q,0)\rangle^2$ is the measured baseline. Note that $g^{(2)}(q,\tau)$ is a defined function. In general, $g^{(1)}(q,\tau)$ is related to the distribution of the characteristic line width $G(\Gamma)$ by[25,26]

$$|g^{(1)}(q,\tau)| = \int_0^\infty G(\Gamma)e^{-\Gamma\tau}\, d\Gamma \qquad (2)$$

For a purely diffusive relaxation, Γ is related to the translational diffusion coefficient D or the cooperative diffusion coefficient D_c by $\Gamma = Dq^2$ or D_cq^2, depending on whether the solution is in the dilute ($C < C^*$) or semidilute ($C > C^*$) regime. On the other hand, it has been shown that, in a semidilute solution or a solution undergoing the cross-linking reaction, $g^{(2)}(q,\tau)$ can also be analyzed by a single-exponential function combined with a stretched exponential function to take care of the additional slow relaxation as follows[27−29]

$$|g^{(1)}(q,\tau)| = A_f \exp\left(-\frac{\tau}{\langle\tau_c\rangle_f}\right) + A_s \exp\left(-\frac{\tau}{\langle\tau_c\rangle_s}\right)^b \qquad (3)$$

where A and $\langle\tau_c\rangle$ are the intensity weighting and the average characteristic decay time, respectively; subscripts "s" and "f" denote the fast and slow modes, respectively; and $0 < b < 1$, a constant related to the distribution width of the characteristic decay time $\langle\tau_c\rangle$ of the slow mode. Note that $A_f + A_s = 1$. Strictly speaking, when using eq 3, we have assumed that the two relaxation modes are "monodisperse", which is not true in reality. We should remember that it is just an approximation. The details of the LLS instrumentation and theory can be found elsewhere.[25,26] The semidilute solution was prepared by dissolving a proper amount of P(MMA-*co*-AMC) in chloroform. The solution was filtered into a quartz LLS cell (10 mm in diameter) to remove dust and sealed under nitrogen. The clarified solution was irradiated in a UV photoreactor equipped with 10 tubes of 310 nm lamps (total energy output of ~150 W) and studied by LLS after different UV-irradiation times.

Results and Discussion

Figure 1 shows that in the initial semidilute solution prior to the photo-cross-linking $g^{(2)}(q,\tau)$ has two distinct relaxation modes. The fast relaxation corresponds to the cooperative diffusion of the subchains between two entangled points, which is well described by the "blob"

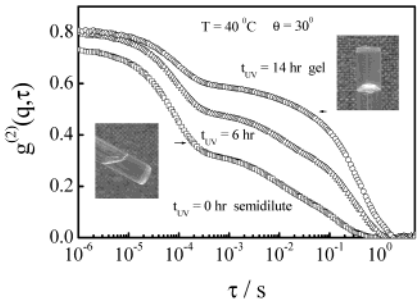

Figure 1. Normalized intensity−intensity time correlation functions of cross-linkable [P(MMA-*co*-AMC)] chains in chloroform during the sol−gel transition.

or scaling theory,[3] while the controversial slow relaxation can be attributed to the thermally agitated density fluctuation of the congested polymer chains.[21,22] As the cross-linking proceeds, the slow relaxation becomes even slower, and at the same time, its contribution to the total scattering intensity increases, reflecting in the raise of its amplitude. The flowing semidilute solution finally becomes a macroscopically immobile chemical gel after ∼9 h UV irradiation, as shown in the insets. Note that even in the gel state $g^{(2)}(q,\tau)$ can still completely relax to zero even the relaxation is fairly slow, indicating that there is no static frozen-in component inside. It is important to note that the complete relaxation of $g^{(2)}(q,\tau)$ is not due to an improper normalization.[30,31] This is because the intercept (β_{app}) of $g^{(2)}(q,\tau)$ at $\tau \rightarrow 0$ increases during the sol−gel transition.

A reasonable explanation of the increase of β_{app} in Figure 1 is as follows. The scattered light intensity comes from solvent (I_s), uncorrelated chain segments or "blobs" (I_{blobs}), and correlated chain segments or "clusters" ($I_{cluster}$); namely, $I_{solution} = I_s + I_{blobs} + I_{cluster}$. Let us not consider the nature of the clusters at this moment. Here, I_s normally contributes so little that it can be neglected. Therefore, the intensity−intensity time correlation function $G^2(q,\tau)$ becomes $\langle[I_{blobs}(q,0) + I_{cluster}(q,0)][I_{blobs}(q,\tau) + I_{cluster}(q,\tau)]\rangle$. The relaxation of the blobs is much faster than that of larger "clusters", evidenced in Figure 1. Therefore, $g^{(2)}(q,\tau)$ is approximated as

$$g^{(2)}(q,\tau) \approx \beta\left[\frac{I_{cluster}}{I_{solution}}\left|g^{(1)}{}_{cluster}(q,\tau)\right|\right]^2 \qquad (4)$$

where for the simplicity of discussion we did not consider the cross-correlation term between the "blobs" and "clusters". In comparison with eq 1, $\beta_{app} = \beta(I_{cluster}/I_{solution})^2$. Initially, $I_{cluster}$ is only a fraction of $I_{solution}$ so that β_{app} is much less than β. As the cross-linking proceeds, $\langle I\rangle_T$ increases ∼10^2 times, mainly due to the increase of $I_{cluster}$ (will be shown later), so that the ratio $I_{cluster}/I_{solution}$ increases. This is why β_{app} approaches β as the cross-linking proceeds. The lack of static frozen-in components is further supported by the sample-position-independent scattering intensity; namely, no speckle was detected when we randomly turned the LLS cell to let the laser hit different parts of the gel.

Figure 2 shows that the time-averaged scattering intensity $\langle I\rangle_T$ randomly fluctuates around the ensemble-averaged scattering intensity $\langle I\rangle_E$, and its distribution roughly follows the Gaussian distribution. There is no obvious speckle. The gel behaves just like an ergodic solution, especially at higher temperatures. It is helpful

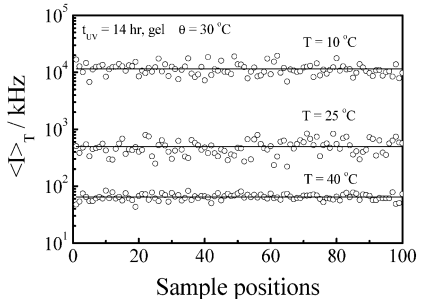

Figure 2. Sample position dependence of total time-averaged scattering intensity $\langle I\rangle_T$ of P(MMA-*co*-AMC) gel at different temperatures. Each solid line represents an ensembly averaged scattering intensity $\langle I\rangle_E$ defined as $(\sum_i \langle I\rangle_{T,i})/N$ with N the total number of randomly chosen sample positions.

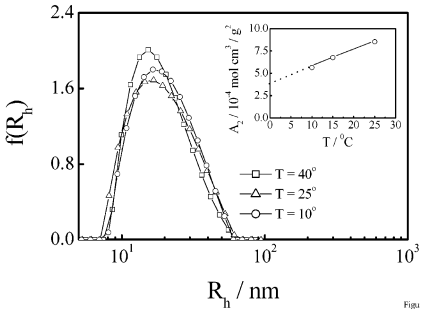

Figure 3. Temperature dependence of hydrodynamic radius distribution of cross-linkable [P(MMA-*co*-AMC)] chains in dilute chloroform solution ($C = 9.0 \times 10^{-4}$ g/mL). The inset shows temperature dependence of second virial coefficient A_2.

to note that in conventional gels the fluctuation of $\langle I\rangle_T$ can be over ∼10^2 times, and the appearing frequency of $\langle I\rangle_T$ monotonically decreases with an increasing $\langle I\rangle_T$.[29] It is clear that as the temperature decreases from 40 to 10 °C, $\langle I\rangle_T$ increases ∼180 times. Conventional wisdom led us to think that this might be due to chain contraction at lower temperatures. However, Figure 3 clearly shows that as the temperature decreases, there is no change in the hydrodynamic radius distribution of the chains in dilution solution. Note that in the calculation of R_h we already corrected the effects of the solvent viscosity and temperature by using the Stokes−Einstein equation. Moreover, the inset shows that chloroform is still a fairly good solvent for the chains even at 10 °C. The extrapolation of $A_2 \rightarrow 0$ reveals that the Θ-temperature is −18 °C, far away from the temperature range studied. Therefore, we cannot attribute the increase of $\langle I\rangle_T$ to the chain contraction. The conventional wisdom is wrong here. We will come back to this point. Let us first analyze each measured $g^{(2)}(q,\tau)$ by the Laplace inversion program (CONTIN) in the correlator to can yield an intensity-weighted distribution of the characteristic decay time $G(\tau_c)$ on the basis of eq 2.

Figure 4 shows the variation of $f(\tau_c)$ from a semidilute solution to a gel network, where $\tau_c = 1/\Gamma$. Note that $f(\tau_c) = \tau_c G(\tau_c)$ because the x-axis is logarithmic. During the sol−gel transition, the bimode distribution is clearly preserved although the relative contribution of the fast relaxation decreases. Shibayama et al.[32] also reported that the fast mode remained in the formation of silica gels. Another interesting point is that the position of the peak related to the fast relaxation nearly remains during the sol−gel transition, different from other gelling systems.[29] The peak related to the slow relaxation progressively shifts to a longer delay time; i.e., the cross-linking slows down the density fluctuation. It

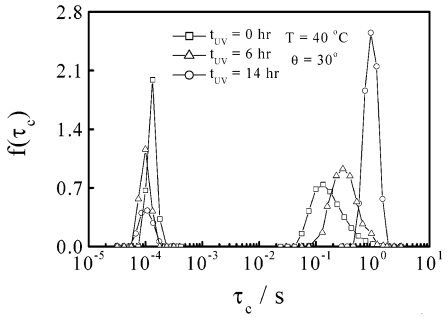

Figure 4. Peak area-normalized intensity distributions of characteristic decay time $f(\tau_c)$ of cross-linkable [P(MMA-*co*-AMC)] chains in chloroform during the sol−gel transition, where $f(\tau_c)$ is τ_c-weighted $G(\tau_c)$, i.e., $f(\tau_c) \equiv \tau_c G(\tau_c)$, because the *x*-axis is logarithmic.

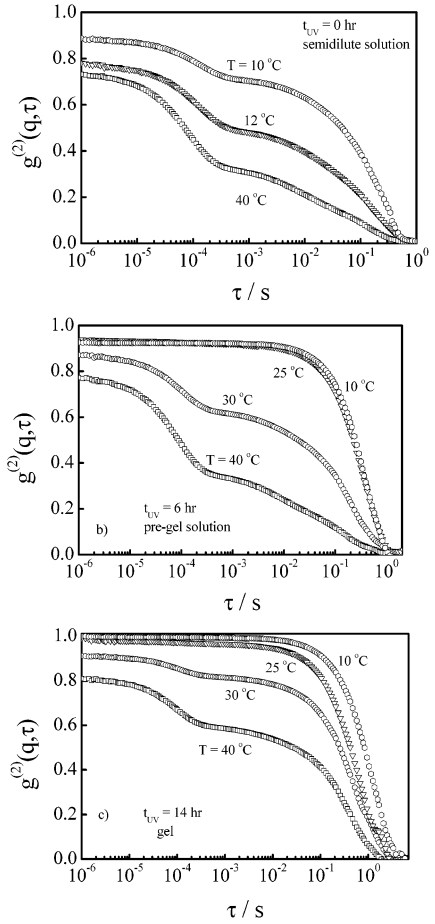

Figure 5. Temperature dependence of normalized intensity−intensity time correlation functions $g^{(2)}(q,\tau)$ of cross-linkable [P(MMA-*co*-AMC)] chains during the sol−gel transition: (a) in semidilute solution, (b) in pregel solution, and (c) in gel.

should be addressed that the cross-linking mostly occurs at the entangled points because only two very nearby coumarin groups can undergo the [2 + 2] photocycloaddition. Therefore, the cross-linking should have a limited effect on the length of the subchains ("blobs"). This explains why the peak related to the fast relaxation remains its position. Next, let us examine how the temperature affects the fast and slow relaxation modes.

Figure 5a shows that in the semidilute solution the intensity contributions of the fast and slow modes (the height of each step) are similar 40 °C. As the temperature decreases, there is nearly no change in the positions of the two relaxation modes, but the intensity

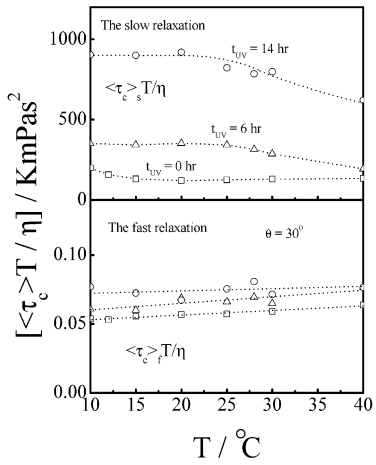

Figure 6. Temperature dependence of fast and slow characteristic decay times ($\langle\tau_c\rangle_f$ and $\langle\tau_c\rangle_s$) of cross-linkable [P(MMA-*co*-AMC)] chains in chloroform during the sol−gel transition, where $\langle\tau_c\rangle_f$ and $\langle\tau_c\rangle_s$ have already been corrected by temperature (T) and solvent viscosity (η).

contribution of the slow mode increases. Note that the intercept of $g^{(2)}(q,\tau)$ at $\tau \rightarrow 0$ increases as the temperature decreases. Some of previous studies suggested that the slow relaxation could be related to the motions of "transient" clusters formed due to the density fluctuation.[11,16,21] In this case, the increase of the scattering intensity related to the slow mode ($\langle I\rangle_{slow}$) can be apparently and qualitatively attributed to the increase of the amplitude (the contrast between the denser and sparser parts) of the density fluctuation. Figure 5b,c reveals that such a temperature effect becomes more dramatic as the cross-linking proceeds, evidenced by the apparent disappearance of the fast relaxation at lower temperatures. To quantitatively extract more information about the two characteristic decay times ($\langle\tau_c\rangle_f$ and $\langle\tau_c\rangle_s$) as well as their intensity weightings contributions (A_f and A_s), we used eq 3 to analyze each measured $g^{(2)}(q,\tau)$ because it is more robust than the Laplace inversion analysis (eq 2), which is more sensitive to the unavoidable experimental noise in the baseline.

Figure 6 shows that before the gelation the temperature and viscosity corrected average characteristic decay time $\langle\tau_c\rangle_f$ of the fast mode is nearly independent of the temperature at different stages of the sol−gel transition, especially in the gel state. This is expected since the fast relaxation is related to the localized motions of the blobs. As for the slow mode, the relaxation in the pregel solution as well as in the gel becomes slightly faster ($\langle\tau_c\rangle_s$ decrease) as the temperature increases but nearly remains in the temperature range 10−20 °C. In the semidilute solution, the relaxation slows down only when the temperature is lower than ∼13 °C. Note that for a given temperature the relaxation, especially for the slow mode, apparently becomes slower as the cross-linking proceeds. Here we only corrected the temperature-dependent solvent viscosity. In principle, we should correct each $\langle\tau_c\rangle$ by the microscopic solution viscosity, a complicated function of both the cross-linking extent and the temperature. The slowdown of the slow relaxation can be attributed to the dumping of the density fluctuation by the cross-linking or higher viscosities at lower temperatures.

Figure 7 shows that the intensity contribution of the fast relaxation (A_f) increases with the temperature, but the trend is quite different with and without the cross-

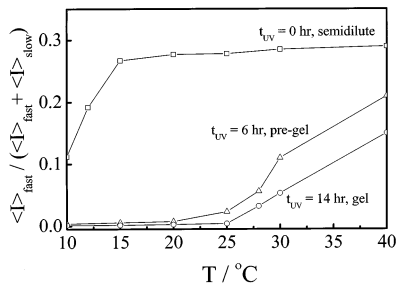

Figure 7. Temperature dependence of intensity weighting (relative contribution) of fast relaxation (A_f) of cross-linkable [P(MMA-*co*-AMC)] chains in chloroform during the sol−gel transition. Note that $A_f + A_s = 1$.

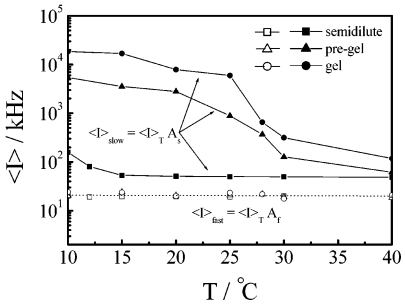

Figure 8. Temperature dependence of time-averaged scattering intensities ($\langle I\rangle_{fast}$ and $\langle I\rangle_{slow}$) related to fast and slow relaxation of cross-linkable [P(MMA-*co*-AMC)] chains in chloroform during the sol−gel transition, where $\langle I\rangle_T$ is overall time-averaged scattering intensity measured in static LLS.

linking. Note that the sum of the two peak areas equals unity, i.e., $A_f + A_s = 1$, so that we only plot A_f vs T. The fast relaxation of the cross-linked chains contributes very little at lower temperatures. It should be noted that the overall time-averaged scattering intensity ($\langle I\rangle_T$) measured in static LLS is the sum of $\langle I\rangle_{fast}$ and $\langle I\rangle_{slow}$. $\langle I\rangle_T$ increases ~180 times as the temperature decreases (Figure 2). Therefore, it is necessary to calculate the average scattering intensities ($\langle I\rangle_{fast}$ and $\langle I\rangle_{slow}$) for the fast and slow modes. The results are shown in Figure 8. It is helpful to note that static and dynamic LLS measurements were done in a back-to-back fashion on the same sample under identical conditions and at the same q. On the basis of Figures 7 and 8, we know that the decrease of A_f is attributed to the increase of $\langle I\rangle_{slow}$. This is understandable because the fast relaxation is related to the motions of the subchains (blobs) between two entangled (cross-linked) points. The temperature should have no effect on the average length of the subchains and the refractive index contrast between the blobs and solvent since the temperature dependence of the refractive index is only on the order of 10^{-4}.

As for the increase of $\langle I\rangle_{slow}$, we should note that in semidilute solution polymer chains are highly entangled with each other. Inside the volume of one chain, there also exist many other chains, especially when the chain is long. Assuming that each chain with a radius of gyration (R_g) has n_s segments and there are n_p chains inside its occupied space (~R_g),[3] the scattering intensity ($\langle I\rangle$) from the $n_s n_p$ segments on the basis of the LLS theory is related the position of each segment (r) as follows:[25]

$$\langle I\rangle_T \propto \langle \sum_{j=1}^{n_s n_p} \sum_{k=1}^{n_s n_p} \exp(i[\vec{q}\cdot(\vec{r}_j - \vec{r}_k)])\rangle \qquad (5)$$

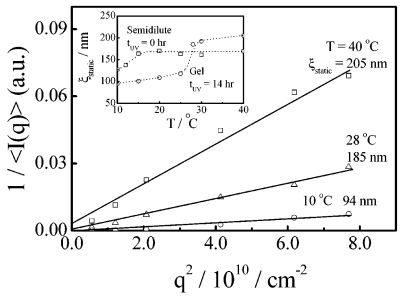

Figure 9. Scattering vector (q) dependence of reciprocal time-averaged scattering intensity $\langle I(q)\rangle$, where the slope-to-intercept ratio leads to the static correlation length (ξ_{static}) on the basis of the on the Ornstein−Zernike equation,[35] [$\langle I(q)\rangle = \langle I(0)\rangle/1 + q^2\xi_{static}^2$], where $\langle I(0)\rangle$ is the scattering intensity at $q \to 0$. The inset shows the temperature dependence of ξ_{static} in initial semidilute solution and resultant gel.

If the motions of $n_s n_p$ segments are fully correlated, $\langle I\rangle_T \propto (n_s n_p)^2$ when $qR_g \ll 1$, while if the motions of $n_s n_p$ segments are completely independent, $\langle I\rangle_T \propto n_s n_p$. In the reality, $\langle I\rangle_T$ is between $n_s n_p$ and $(n_s n_p)^2$ in semidilute solution because the segments between different chains are only partially correlated. The cross-linking makes the segments between different chains more correlated so that the scattering intensity increases. On the other hand, the increase of the solution viscosity at lower temperatures enhances the hydrodynamic interaction of the segments between different chains. This explains the increase of $\langle I\rangle_{slow}$ with a decreasing temperature.

It has been known that ξ_{static} inside a semidilute solution or a gel network can be related to the scattering light intensity ($I(q)$) and the scattering vector (q) by the Ornstein−Zernike equation.[33,34]

$$I(q) = \frac{I(q \to 0)}{1 + q^2\xi_{static}^2} \qquad (6)$$

Figure 9 shows that the static correlation length (ξ_{static}) of the density fluctuation of the gel network has a length scale over ~10^2 nm. The inset shows that in the gel ξ_{static} increases with the temperature, and there is a large change between 25 and 30 °C, while in semidilute solution ξ_{static} only decreases when the temperature is lowered to ~13 °C. The decrease of ξ_{static} can be attributed to the increases of the solution viscosity and modulus. On the other hand, Figure 8 shows that $\langle I\rangle_{slow}$ decreases ~180 times during the same temperature change. Therefore, a combination of the increase of $\langle I\rangle_{slow}$ and the decrease of ξ_{static} excludes the possible attribution of the slow relaxation to some physically associated chains clusters[11] or an incomplete dissolution.[1,13] This is because chloroform remains a good solvent, and there is no chain contraction in the temperature range studied. Next, let us examine how the temperature affects the scattering vector (q) dependence of the line widths ($\Gamma_f = 1/\langle\tau_c\rangle_f$ and $\Gamma_s = 1/\langle\tau_c\rangle_s$) at different stages of the sol−gel transition.

Figure 10 shows that at 25 °C Γ_f is scaled to q as $\Gamma_f \sim q^{\alpha_f}$ with $\alpha_f = 2.0 \pm 0.1$ in the semidilute solution, revealing a pure cooperative diffusive relaxation. As the cross-linking proceeds, α_f increases to 2.4 because the motions of different "blobs" become less independent, particularly in the gel state. On the other hand, in the semidilute solution, the scaling exponent α_s between Γ_s and q is 3.0 ± 0.1. This is because the dimension of the density fluctuation ($\xi_{static} \sim 170$ nm) is larger than the

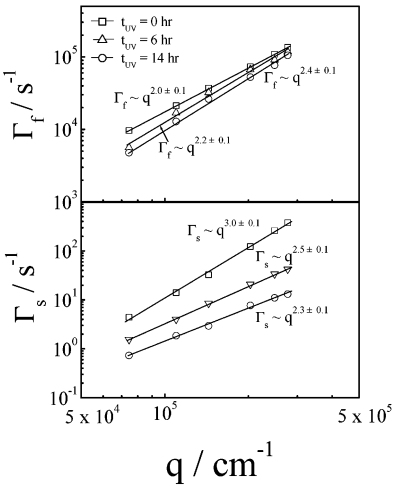

Figure 10. Scattering vector (q) dependence of average characteristic line widths ($\Gamma_f = 1/\langle\tau_c\rangle_f$ and $\Gamma_s = 1/\langle\tau_c\rangle_s$) of fast and slow relaxation of cross-linkable [P(MMA-*co*-AMC)] chains in chloroform during the sol−gel transition.

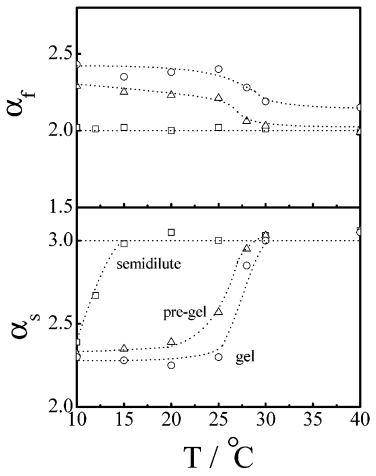

Figure 11. Temperature dependence of scaling exponents (α_f and α_s) in $\Gamma_f \sim q^{\alpha_f}$ and $\Gamma_f \sim q^{\alpha_s}$ for fast and slow relaxation of cross-linkable [P(MMA-*co*-AMC)] chains in chloroform during the sol−gel transition.

LLS observation length $1/q$ used so that the light probes the internal motions. As the cross-linking proceeds, ξ_{static} becomes comparable to $1/q$, and the light probes only part of the internal motions so that α_s decreases from 3.0 to 2.3, similar to the study of a long linear polymer chain or spherical swollen microgel when $1/q$ is comparable to the size of the chain or microgel.[35,36]

On the basis of the above discussion, we would expect a decrease of α_f and an increase of α_s as the temperature increases because the decrease of the solution viscosity at higher temperatures will make the motions of different blobs more independent and, at the same time, increase the dimension of the density fluctuation (not due to the swelling, but less dumping). Figure 11 shows exactly what we have expected. In the semidilute solution, α_f is independent of the temperature, while α_s drops only when the temperature is lower than ∼13 °C, which agrees well with the decrease of ξ_{static} at ∼13 °C, as shown in the inset of Figure 9. In the pregel solution as well as in the gel, both α_f and α_s remain constants when the temperature is higher than 30 °C, which also agrees with the constant ξ_{static} in the same temperature range, as shown in the inset of Figure 9. For the gel at 40 °C, ξ_{static} is longer than $1/q$ so that the lights probe

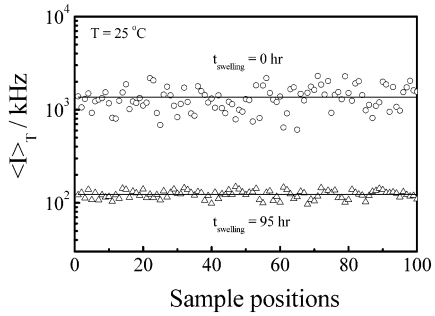

Figure 12. Effect of swelling on sample position dependence of time-averaged scattering intensity $\langle I\rangle_T$, where each solid line represents an ensembly averaged scattering intensity $\langle I\rangle_E$ defined as $(\sum_i \langle I\rangle_{T,i})/N$, with N the total number of randomly chosen sample positions.

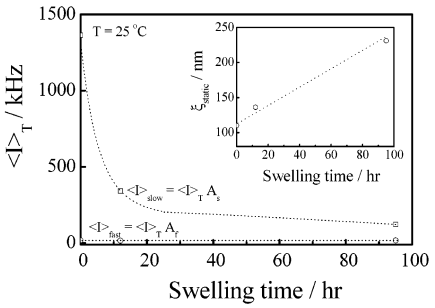

Figure 13. Effect of swelling on time-averaged scattering intensities ($\langle I\rangle_{fast}$ and $\langle I\rangle_{slow}$) related to fast and slow relaxation of P(MMA-*co*-AMC) gel, where $\langle I\rangle_T$ is overall time-averaged scattering intensity measured in static LLS. The inset shows the effect of swelling on the static correlation length (ξ_{static}) calculated on the basis of Ornstein−Zernike equation [$\langle I(q)\rangle = \langle I(0)\rangle/(1 + q^2\xi_{static}^2)$].

the internal motions and α_s approaches ∼3.0. As discussed before, when ξ_{static} becomes comparable to $1/q$, the light probes only part of the internal motions, resulting in the decrease of α_s. The above discussion is further supported by the following swelling experiment.

Figures 12 and 13 show that as the swelling proceeds, it is the decrease of $\langle I\rangle_{slow}$ that leads to the decrease of the total scattering intensity $\langle I\rangle_T$. Considering that the gel volume swells only ∼2 times, we would expect a similar decrease of $\langle I\rangle_T$ if the segments of different chains are not correlated. However, Figure 12 shows that $\langle I\rangle_T$ decreases ∼11 times, indicating that the swelling reduces not only the chain concentration in the scattering volume but also the correlation of the lights scattering from the segments of different chains. The inset in Figure 13 reveals that the swelling leads to an increase of the static correlation length (ξ_{static}) from 110 to 230 nm. This is because the swelling increases the chain dimension and reduces the viscosity.

Figure 14 shows that the swelling has no effect on the characteristic decay rate $\langle\tau_c\rangle_{fast}$ of the fast relaxation. Note that for a given temperature $\langle\tau_c\rangle_{fast}$ is proportional to the viscosity (η) and the dynamic correlation length (the mesh size) $\xi_{dynamic}$. The swelling increases $\xi_{dynamic}$ but decreases η. The constant $\langle\tau_c\rangle_{fast}$ reveals that the swelling effects on $\xi_{dynamic}$ and η are somehow canceled. On the other hand, the swelling makes the slow relaxation faster ($\langle\tau_c\rangle_{slow}$ decreases). This is understandable because the swelling decreases the viscosity and increases the frequency of the density fluctuation of the gel network. The inset in Figure 14 shows the expected results, namely, the swelling leads to the increase of the scaling exponent α_s in $1/\langle\tau_c\rangle_s \sim q^{\alpha_s}$ from 2.3 ± 0.1 to

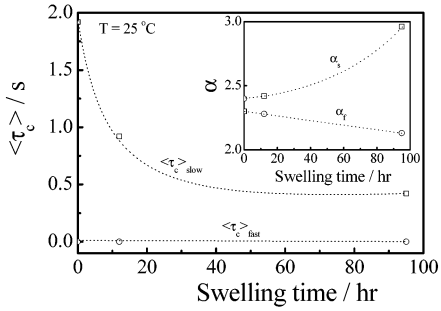

Figure 14. Effect of swelling on fast and slow characteristic decay times ($\langle\tau_c\rangle_f$ and $\langle\tau_c\rangle_s$) of P(MMA-*co*-AMC) gel. The inset shows the effect of swelling on scaling exponents α_f and α_s in $1/\langle\tau_c\rangle_{fast} \propto q^{\alpha_f}$ and $1/\langle\tau_c\rangle_{slow} \propto q^{\alpha_s}$, where q is the scattering vector.

3.0 ± 0.1, supporting our previous discussion that variation of $2 \leq \alpha_s \leq 3$ depends on whether the LLS observation length ($1/q$) is smaller than, comparable to, or larger than the dimension of the density fluctuation (ξ_{static}). On the other hand, the fact that $\alpha_f > 2$ shows that the fast relaxation of the gel network is not purely diffusive because in comparison with the semidilute solution the cross-linking in the gel network makes the blobs less independent.

Conclusion

The incorporation of photo-cross-linkable functional group 7-methacryloyloxy-4-methylcoumarin (AMC) into poly(methyl methacrylate) (PMMA) chains enables us to control the transition from a semidilute solution to a homogeneous and speckle-free chemical gel. The studies of the chain conformation and solvent quality in dilute solutions reveal that chloroform remains a good solvent in the temperature range 10−40 °C, and there is no chain contraction even at 10 °C. The dynamic laser light scattering (LLS) shows that the fast and slow relaxation modes observed in the semidilute solution are preserved during the sol−gel transition. The average characteristic decay time $\langle\tau_c\rangle_f$ of the fast relaxation and its related scattered light intensity are nearly independent of the temperature. This is expected because the temperature should have no significant effect on the average length of the subchains (blobs) between two entangled (cross-linked) points or the refractive index contrast between the subchains and solvent. On the other hand, the scattering intensity related to the slow relaxation ($\langle I\rangle_{slow}$) increases with a decreasing temperature. This is because the viscosity increases at lower temperature so that the lights scattered from the segments of different entangled (cross-linked) chains become more correlated. The line widths ($\Gamma_f = 1/\langle\tau_c\rangle_f$ and $\Gamma_s = 1/\langle\tau_c\rangle_s$) of these two modes can be scaled to the scattering vector q as $\Gamma_f \sim q^{\alpha_f}$ and $\Gamma_s \sim q^{\alpha_s}$, respectively. As the temperature decreases, α_f increases, but α_s decreases, in the pregel solution as well as in the gel. The increase of α_f can be attributed to less independent motions of different blobs at lower temperatures, while the decrease of α_s is due to the decrease of the static correlation length (ξ_{static}); namely, ξ_{static} becomes comparable to the LLS observation length $1/q$ at lower temperatures so that the light probes only part of the internal motions. The swelling of the resultant gel has a similar effect as the increase of the temperature. The effects of the temperature and swelling on the fast and slow modes confirm that the fast relaxation observed during the sol−gel transition is related to the cooperative motions (not purely diffusion as previously thought) of the subchains (blobs) between two entangled or cross-linking points, and the controversial slow relaxation is due to the thermally agitated density fluctuation. The variation of the scaling exponent α_s in $\Gamma_s \sim q^{\alpha_s}$ is indeed attributed to the relative length of the dimension (ξ_{static}) of the density fluctuation to the LLS observation length ($1/q$).

Acknowledgment. The financial support of NNSF Project (20274045), the Hong Kong Special Administration Region Earmarked Grants (CUHK4257/00P, 2160174), the Special Funds for Major State Basic Research Projects (G1999064800), and the CAS Bai Ren Project is gratefully acknowledged.

References and Notes

(1) Stepánek, P.; Brown, W. *Macromolecules* **1998**, *31*, 1889. Brown, W.; Nicolai, T. *Colloid Polym. Sci.* **1990**, *268*, 977. In *Dynamic Light Scattering, the Methods and Application*; Brown, W., Ed.; Clarendon: Oxford, 1993; p 273.
(2) Teraoka, I. *Polymer Solutions An introduction to Physical Properties*; John Wiley & Sons: New York, 2002; p 277.
(3) de Gennes, P. G. *Scaling Concepts in Polymer Physics;* Cornell University Press: Ithaca, NY, 1979. Daoud, D.; Cotton, J. P.; Farnoux, B.; Jannink, G.; Sarma, G.; Beboit, J.; Duplessix, C.; Picot, C.; de Gennes, P. G. *Macromolecules* **1975**, *8*, 804. Doi, M.; Edwards, S. F. *The Theory of Polymer Dynamics*, Oxford Press: New York, 1986.
(4) Chu, B.; Nose, T. *Macromolecules* **1980**, *13*, 122.
(5) Amis, E. J.; Han, C. C.; Matsushita, Y. *Polymer* **1984**, *25*, 650.
(6) Brown, W.; Johnsen, R. M.; Stepanek, P.; Jakes, J. *Macromolecules* **1988**, *21*, 2859.
(7) Adam, M.; Delsanti, M. *Macromolecules* **1985**, *18*, 1760.
(8) Brown, W.; Stepanek, P. *Macromolecules* **1988**, *21*, 1791; **1993**, *26*, 6884. Nicolai, T.; Brown, W.; Johnson, R. M.; Stepanek, P. *Macromolecules* **1990**, *23*, 1165.
(9) Faraone, A.; Magazu, S.; Maisano, G.; Ponterio, R.; Villari, V. *Macromolecules* **1999**, *32*, 1128.
(10) Koch, T.; Strobl, G. R.; Stuhn, B. *Polymer* **1993**, *34*, 1988.
(11) Heckmeier, M.; Mix, M.; Strobl, G. *Macromolecules* **1997**, *30*, 4454.
(12) Fleischer, G. *Macromolecules* **1999**, *32*, 2382.
(13) Burchard, W. *Trends Polym. Sci.* **1993**, *1*, 192.
(14) Ermi, B. D.; Amis, E. J. *Macromolecules* **1998**, *31*, 7378.
(15) Tanahatoe, J. J.; Kuil, M. E. *J. Phys. Chem. B* **1997**, *101*, 9233, 10839.
(16) Konak, C.; Helmstedt, M.; Bansil, R. *Macromolecules* **1997**, *30*, 4342; **1998**, *31*, 4639.
(17) Tsunashima, Y.; Kawanishi, H.; Nomura, R.; Horii, F. *Macromolecules* **1999**, *32*, 53.
(18) Esquenet, C.; Buhler, E. *Macromolecules* **2002**, *35*, 3708.
(19) Klucker, R.; Munch, J. P.; Schosseler, F. *Macromolecules* **1997**, *30*, 3839.
(20) Esquenet, C.; Buhler, E. *Macromolecules* **2001**, *34*, 5287.
(21) Ngai, T.; Wu, C. *Macromolecules,* **2003**, *36*, 848.
(22) Ngai, T.; Wu, C.; Chen, Y. *Macromolecules,* submitted for publication.
(23) Chen, Y.; Wu, J.-D. *J. Polym. Sci., Polym. Chem. Ed.* **1994**, *32*, 1867.
(24) Chen, Y.; Geh, J.-L. *Polymer* **1996**, *37*, 4481.
(25) Berne, B. J.; Pecora, R. *Dynamic Light Scattering;* Plenum Press: New York, 1976.
(26) Chu, B. *Laser Light Scattering*, 2nd ed.; Academic Press: New York, 1991.
(27) Adam, M.; Delsanti, M.; Munch, J. P.; Durand, D. *Phys. Rev. Lett.* **1988**, *61*, 706.
(28) Martin, J. E.; Wilcoxon, J. *Phys. Rev. Lett.* **1988**, *61*.373.
(29) Shibayama, M. *Macromol. Chem. Phys.* **1998**, *199*, 1. Shibayama, M.; Norisuye, T. *Bull. Chem. Soc. Jpn.* **2002**, *75*, 641.
(30) Moussaid, A.; Munch, J. P.; Schosseler, F.; Candau, S. J. *J. Phys. II* **1991**, *1*, 637.
(31) Krall, A. H.; Huang, Z.; Weitz, D. A. *Physica A* **1997**, *235*, 19.
(32) Norisuye, T.; Inoue, M.; Shibayama, M.; Tamaki, R.; Chujo, Y. *Macromolecules* **2000**, *33*, 900.
(33) Bueche, F. *J. Colloid Interface Sci.* **1970**, *33*, 61.
(34) Soni, V. K.; Stein, R. S. *Macromolecules* **1990**, *23*, 61.
(35) Wu, C.; Chan, K. K.; Xia, K.-Q. *Macromolecules* **1995**, *28*, 1032.
(36) Wu, C.; Zhou, S. Q. *Macromolecules* **1996**, *29*, 1574.

MA030421B